analytical chemistry

Article

pubs.acs.org/ac

Shiga-Like Toxin B Subunit of *Escherichia coli* as Scaffold for High-Avidity Display of Anti-immunocomplex Peptides

Gabriel Lassabe, Martín Rossotti, Andrés González-Techera, and Gualberto González-Sapienza*

Cátedra de Inmunología, Facultad de Química, Instituto de Higiene, UDELAR, Montevideo, Uruguay

Supporting Information

ABSTRACT: Small compounds cannot bind simultaneously to two antibodies, and thus, their immunodetection is limited to competitive formats in which the analyte is indirectly quantitated by measuring the unoccupied antibody binding sites using a competing reporter. This limitation can be circumvented by using phage-borne peptides selected for their ability to specifically react with the analyte−antibody immunocomplex, which allows the detection of these small molecules in a noncompetitive format (PHAIA) with increased sensitivity and a positive readout. In an effort to find substitutes for the phage particles in PHAIA, we explore the use of the B subunit of the Shiga-like toxin of *Escherichia coli*, also known as verotoxin (VTX), as a scaffold for multivalent display of anti-immunocomplex peptides. Using the herbicides molinate and clomazone as model compounds, we built peptide−VTX recombinant chimeras that were produced in the periplasmic space of *E. coli* as soluble pentamers, as confirmed by multiangle light scattering analysis. These multivalent constructs, which we termed nanopeptamers, were conjugated to a tracer enzyme and used to detect the herbicide−antibody complex in an ELISA format. The VTX−nanopeptamer assays performed with over a 10-fold increased sensitivity and excellent recovery from spiked surface and mineral water samples. The carbon black-labeled peptide−VTX nanopeptamers showed great potential for the development of a lateral-flow test for small molecules with a visual positive readout that allowed the detection of up to 2.5 ng/mL of clomazone.

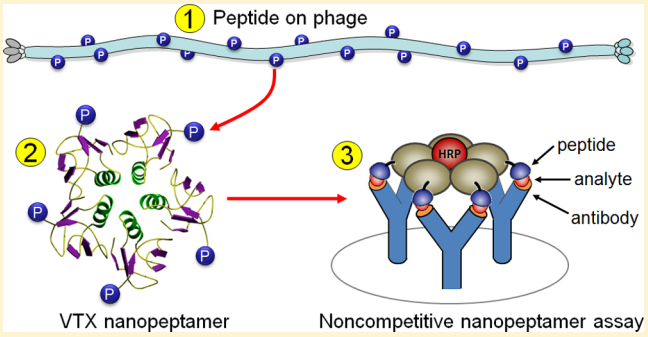

The immunodetection of low molecular mass substances holds great promise for rapid detection of a vast number of small analytes of clinical, toxicological, or environmental interest. Technically, the preferred format would be a two-site noncompetitive assay based on the use of capture and detection antibodies, which is the standard sandwich-type assay used for macromolecular analytes. This format allows the use of an excess amount of antibody driving the antigen−antibody reaction, even in the presence of trace amounts of analyte, thus providing high assay sensitivity.[1] In addition, the two-site recognition "double-checks" that the right target analyte is being detected, maximizing the assay specificity. Unfortunately, high affinity antibodies bind small compounds (immunologically referred to as haptens) in deep pockets that bury most of their surface.[2,3] Upon formation of the hapten−antibody immunocomplex (IC), there is no room for the binding of a second antibody, and thus, these compounds are almost exclusively detected by using competitive immunoassays. To optimize the competition, limiting amounts of reagents need to be used, curbing the assay sensitivity. Previously, we have shown that by using small peptide loops, it was possible to focus the recognition of the IC to the changes produced at the binding pocket upon binding of the hapten.[4] These peptides are selected from phage display libraries upon panning with the desired IC, and the phage-borne peptides can then be used to develop noncompeptive phage anti-immunocomplex assays (PHAIA).

Applied to different small compounds, the PHAIA assay provided and increased sensitivity when compared with the competitive format performed with the same antihapten antibody,[4−6] and improved specificity.[7] Behaving as robust and versatile assay components,[8] the phage particles are unconventional reagents for the immunoassay industry, and their biological nature can become a safety issue. Although synthetic monovalent peptides cannot substitute for the phage-borne peptide, we recently demonstrated that the complexes of commercial streptavidin or avidin with biotinylated anti-immunocomplex synthetic peptides do, showing assay parameters similar to those of the PHAIA.[9]

To explore additional scaffolds for multivalent display of these peptides, we thought of using the Shiga-like toxin, which has a pentameric structure. The Shiga-like toxin B-1 of *Escherichia coli*, also known as verotoxin (VTX) is a highly potent exotoxin that enters host cells and inhibits protein synthesis. It is the smallest of the AB_5 bacterial toxin family, which consists of an active A subunit associated with a

Received: March 12, 2014
Accepted: May 6, 2014
Published: May 6, 2014

   dx.doi.org/10.1021/ac500926f | *Anal. Chem.* 2014, 86, 5541−5546

pentamer of receptor-binding B subunits.[10] The recombinant B subunit of VTX has been shown to oligomerize in a doughnut-like pentamer[11] that is fully capable of host cell binding in the absence of the A subunit.[12] There are two isoforms of the nontoxic subunit, B-1 and B-2 that share 57% identity. The 7.7 kDa B-1 subunit forms more stable oligomers[13] and has been used to increase the avidity of monodomain antibodies selected from phage libraries.[14,15] The use of the B subunit as a scaffold for multivalent display is facilitated by the fact that its N-terminus is exposed to the solvent and radiates out from the periphery of the pentamer core (Figure 1), and in addition, recombinant VTX and VTX chimeric proteins are produced in *E. coli* with high yield (tens of milligrams per liter of culture).[14]

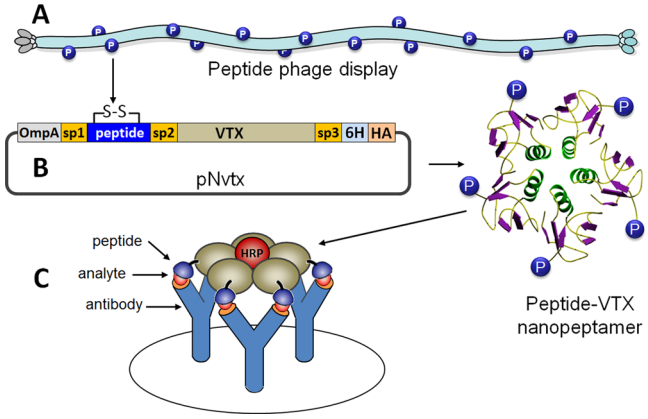

Figure 1. Nanopeptamer assay using verotoxin for multivalent display of anti-immunocomplex peptides isolated by phage display. (A) Once the anti-immuncomplex peptide is selected from phage libraries, (typically displayed on the major capside protein pVIII), its coding sequence is cloned into the pNvtx vector (B) fused to the VTX gene. The OmpA signal peptide is used for periplasmic expression of the peptide−VTX nanopeptamer monomers, which spontaneously oligomerize, forming the pentavalent nanopeptamer. (C) The high avidity of the recombinant nanopeptamer conjugated to peroxidase (HRP) can then be used to detect the formation of the immunocomplex, in a two-site antibody−nanopeptamer immunoassay.

In this work, we built VTX-based nanopeptamers using anti-immunocomplex peptides selected against the herbicides molinate and clomazone bound to their cognate antibodies. These nanopeptamers were produced at high yields as soluble recombinant proteins and showed assay performances similar to the respective phage-borne peptides.

MATERIALS AND METHODS

Materials. Mouse IgG monoclonal antibodies (mAb) 14D7 and 5.6 against molinate and clomazone, respectively, were prepared as described before.[16,17] Molinate was a gift from Stauffer Chemical Co, and clomazone was purchased from Riedel-de Haën, Seelze, Germany. Protein G affinity, BPER (bacterial protein extraction reagent), AminoLink reductant sodium cyanoborohydride and horseradish peroxidase (HRP) were purchased from Pierce (Rockford, IL). NAP-5 columns prepacked with Sephadex G-25, molecular weight markers, and the Superose 12HR 10/30 column were from GE Healthcare (Buckinghamshire, UK). Amicon Ultra centrifugal filters and other common filters were purchased from Millipore (Billerica, MS). The anti-HA-peroxidase antibody and Complete Protease Inhibitor Cocktail were from Roche Diagnostics (Indianapolis). High performance pigment carbon black JY-101P was a kind gift from Hangzhou Juychem Co. (Zhejiang, China). The BCA (Bicinchoninic Acid Kit) for protein determination, bovine serum albumin (BSA), Tween 20, IPTG (isopropyl β-D-1-thiogalactopyranoside), poly(ethylene glycol) 8000 (PEG), 3,3′,5,5′-tetramethylbenzidine (TMB), and other common chemicals were purchased from Sigma (St. Louis, MO).

Assembling of the Anti-immunocomplex Nanopeptamer Genes in the pNvtx Vector. To build the pNvtx vector (Figure 1), the peptide pA-VTX cassette shown in (Figure S-1A of the Supporting Information) was synthesized by Integrated DNA Technologies (IDT, Coralville, IA, USA). This cassette codes for the peptide pA (CSLWDTTGWC), which is specific for the molinate-mAb 14D7 immunocomplex,[4] and the verotoxin-B subunit lacking the signal sequence (amino acid sequence 21−89, EMBL M16625: nt 1349−1555). Peptide pA is flanked by the N-terminal sequence GTASGSA− and is tethered to the N-terminus of the VTX subunit by the −LQGGGSGGGS− spacer. The pNvtx vector was built by digestion of the two noncomplementary SfiI sites of the cassette and its subsequent cloning into a modified pET28a+ vector (Novagen) between the OmpA signal peptide and the 6 × His and HA (hemeagglutinin) tags (Figure 1). The *Kpn*I and *Pst*I restriction sites were engineered to allow for the substitution of the anti-immunocomplex peptide in the pNvtx vector. To this end, two complementary oligonucleotides encoding the new peptide sequence are used, which upon annealing produced the DNA insert with the corresponding overhangs for its cloning with these two enzymes. The pairs of oligonucleotides used in this study for cloning of three anti-immunocomplex peptides specific for the clomazone−mAb 5.6 complex are shown in Figure S-2 of the Supporting Information. All vectors were electroporated in competent BL21(DE3) *E. coli* cells (Life Technologies, Carlsbad, CA, USA).

Expression and Purification of the VTX Nanopeptamers. Small cultures of individual colonies of BL21(DE3) *E. coli* cells, transformed with the peptide-VTX constructions, were grown to check for DNA sequence and expression of the chimera. Selected colonies were used for large-scale production of the nanopeptamers by growing them in 500 mL of LB kanamycin (50 μg/mL) at 37 °C, with shaking at 250 rpm, to an absorbance of 0.5 AU at 600 nm. The cultures where then induced with 1 mM IPTG, incubated for 3 h and centrifuged at 5000*g* for 15 min at 4 °C. The periplasmic extracts were prepared as described by Olichon et al.[18] Briefly, the cell pellets were resuspended in 10 mL of 200 mM Tris, 20% sucrose, 0.5 mM EDTA and pH 8.0 TES buffer and were frozen at −80 °C and thawed to room temperature. After that, 5 mL of TES buffer was added, and the resulting solutions were incubated for 30 min on ice and further diluted with 3 mL of TES and 12 mL of H_2O. After 30 min on ice, the extracts were centrifuged at 30 000*g* for 20 min at 4 °C. The supernatants were supplemented with NaCl and imidazole up to 0.3 M and 20 mM, respectively, and directly used for purification. To this end, 30 mL of this periplasmic extract was applied to a Ni-NTA column (HisTrap HP 1 mL, GE Health Care, Pittsburgh, USA) equilibrated with a buffer of 50 mM Na_2HPO_4, 0.3 M NaCl, 20 mM imidazol, pH 8. The column was then washed with 5 column volumes of the same buffer, and the protein was eluted (1 mL fractions) by increasing the concentration of imidazole to 500 mM. After dialysis against PBS, the recombinant nanopeptamers were supplemented with Complete Protease Inhibitor Cocktail and sodium azide 0.05%. The protein concentration was

dx.doi.org/10.1021/ac500926f | *Anal. Chem.* 2014, 86, 5541−5546

determined using the BCA kit, and the preparation was filtered (0.22 μm) and stored in aliquots at −80 °C until used.

Analysis of the Oligomeric Status of the Nanopeptamers by Size-Exclusion Chromatography (SEC) and Online Multiangle Light-Scattering (MALLS). The MWs of the nanopeptamers were determined by SEC-FPLC coupled with an UV detector (SPD-20A, Shimadzu), a refractive index detector (RID-10A; Shimadzu), and a three-angle SEC-MALLS/RI (size-exclusion multiangle laser light scattering/refractive index) detector (Wyatt Technologies, Goleta, CA) using a Superose 12 HR 10/30 column (GE Health Care, Pittsburgh) run with phosphate buffer saline, pH 7.5 (PBS), at a flow rate of 0.5 mL/min. The VTX nanopeptamer (2 mg/mL) was applied to the column, and the elution was monitored with UV, IR, and MALLS detectors. The MW standard proteins chymotrypsin (2 mg/mL, 24.8 kDa), ovalbumin (OVA 2 mg/mL, 44.3 kDa), and BSA (2 mg/mL, 66.5 kDa) were used to build an elution-time calibration curve using the IR and UV detectors. BSA was also employed as a calibration protein for the MALLS detector system. The absolute MW calculations with MALLS were performed using a refractive index increment, dn/dc, of 0.186 mL/g.[19] All data were collected and processed with ASTRA software (v4.73.04, Wyatt Technology, Goleta, CA).

Nanopeptamer ELISA for Molinate and Clomazone. Microtiter plates were coated with the appropriate amount of antibody in PBS (optimized by checkerboard titration) for 1 h at 37 °C, blocked with PBS−BSA 1% at 37 °C for 30 min, and washed three times with PBS 0.05% Tween 20 (PBST). Wells were dispensed with 50 μL of the herbicide standards in PBS or water samples plus 50 μL of the optimized dilution of the nanopeptamer-HRP conjugate (Supporting Information) in PBST. After 1 h of incubation and washing, 100 μL of the peroxidase substrate (0.4 mL of 6 mg/mL 3,3′,5,5′-tetramethylbenzidine in DMSO, 0.1 mL of 1% H_2O_2, in 25 mL of 0.1 M citrate acetate buffer, pH 5.5) was added to each well, and the reaction was stopped after 10 min by addition of 50 μL of 2 N H_2SO_4. Absorbance was read at 450/650 nm in a microtiter plate reader (Multiskan MS, Thermo Labsystems, Waltham, MA). For the analysis of field samples, the reaction mix was supplemented with 20% of interference buffer (1 M Tris, 0.3 M NaCl, 0.3 M EDTA, 1% BSA, pH 7.4).

Carbon Black Nanopeptamer Labeling. A 5% solution of carbon black in Milli-Q water was homogenized in a sonication water bath and was then diluted 25-fold with 5 mM boric buffer, pH 8.8. A 120 μg portion of nanopeptamer in 5 mM boric buffer, pH 8.8 (about 100 μL), was combined with 900 μL of the 0.2% carbon black solution and incubated for 3 h at room temperature. The suspension was then centrifuged at 14 000 rpm for 15 min, and the pellet was resuspended in 1 mL of 100 mM boric buffer, pH 8.8 and 0.05% Tween 20 by sonication. After repeating this step three more times, the carbon-labeled nanopeptamer was resuspended in 1 mL of 100 mM boric buffer, pH 8.8; 0.05% Tween 20; and BSA 1% and kept at 4 °C until used. The same procedure was used for labeling a single domain antibody (VHH) fused to the HA tag that was used as the positive control.

Lateral Flow Immunochromatography. mAb 5.6 and anti-HA tag antibody lines were printed on Hi-Flow Plus 120 nitrocellulose membrane cards at 0.30 μg/cm using a BioDot AD 1500 liquid dispenser (BioDot, CA). A 50 μL portion of PBS 0.1% Tween 20 supplemented with 1 μL of the carbon black nanopeptamer and control VHH suspensions was dispensed in microtiter wells and mixed with 50 μL of PBS 0.1% Tween 20 containing different concentrations of clomazone. Strips cut from the printed cards (4 mm) were dipped into the wells and allowed to develop for 20 min.

RESULTS AND DISCUSION

Cloning and Expression of Recombinant Verotoxin B Subunit As Fusion Protein. Figure 1 shows a general scheme of the generation of the VTX nanopeptamers and their use as immunoassay reagents. To assess the functionality of VTX as a scaffold for high-avidity display of anti-immunocomplex peptides, we initially assembled the peptide pA-VTX construct into the pNvtx vector (Figure 1). Peptide pA has been previously isolated from a phage library panned against the immunocomplex (IC) of the herbicide molinate with mAb 14D7. It reacts specifically with the IC but not with the uncombined antibody, allowing the sensitive detection of the herbicide in the PHAIA format.[4] Preliminary experiments of expression of the pA-VTX chimera in IPTG-induced *E. coli* BL21(DE3) showed that the fusion protein occurred as a single SDS-gel band of ∼13 kDa, which is in agreement with the estimated MW of the pA-VTX monomer (12 840 Da). A large portion of the fusion protein was found in the insoluble fraction, but still a significant amount was soluble (Figure 2).

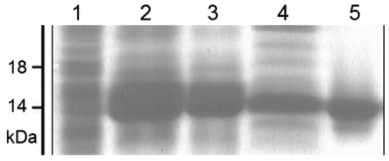

Figure 2. pA-VTX nanopeptamer expression analysis in coomassie-stained SDS-PAGE gels. Total extract of nontransformed (1) and induced (2) cells, insoluble fraction (3), soluble fraction (4), and Ni-NTA purified nanopeptamer (5).

For practical reasons and because of good yields (about 10 mg per liter of culture), we decided to work with this soluble fraction, from which the nanopeptamers were purified by immobilized metal affinity chromatography (Figure 2).

The pA-VTX Nanopeptamer Adopts a Pentameric Structure in Solution. The oligomerization of the recombinant nanopeptamers was studied by size-exclusion chromatography using online light scattering, UV, and refraction index (RI) detectors (SEC-MALLS-RI). pA-VTX eluted as a single symmetric peak at 12.4 mL (Figure 3a), which by comparison with the protein standards corresponds to an apparent MW of 64 kDa, being in good agreement with the calculated MW of 64 205 kDa for the pentameric structure of pA-VTX. This was confirmed, independently of hydrodynamic considerations, by the SEC-MALLS analysis. The molecular mass curve obtained with this method showed a homogeneous distribution of molecular masses along the elution of the pA-VTX peak, with an average value of 64 kDa (Figure 3b). This confirms that in solution, the conformational state of the nanopeptamer is that of a homogeneous pentameric structure, with light dispersion properties corresponding to a monodisperse protein.

The pA-VTX-Nanopeptamer Allowed the Sensitive Detection of Molinate. Once the pentameric nature of the nanopeptamer was established, we confirmed its reactivity against the molinate/mAb 14D7 immunocomplex by ELISA using the HA tag for detection (data not shown). Then, to simplify its use as immunoassay reagent, the purified nano-

dx.doi.org/10.1021/ac500926f | *Anal. Chem.* 2014, 86, 5541−5546

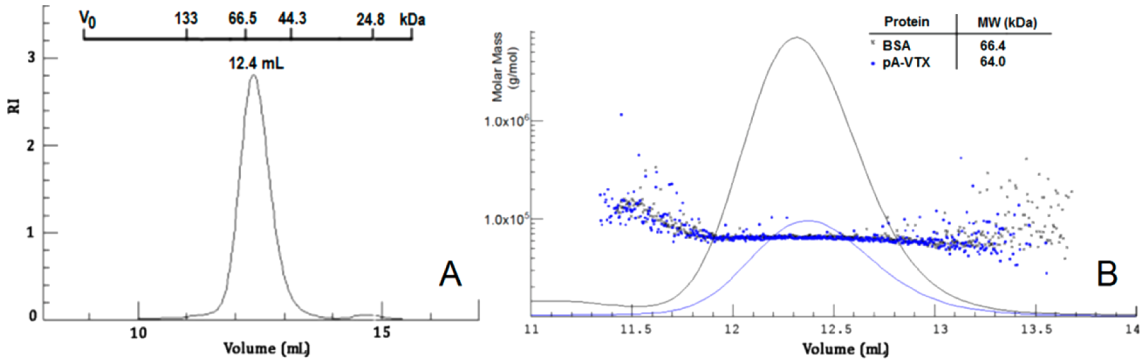

Figure 3. Solution behavior of the pA-VTX nanopeptamer. (A) Size-exclusion chromatogram of the nanopeptamer on a Superose 12 column (RI = refractive index). The elution volume of pA-VTX (12.4 mL) was compared with that of standard proteins corresponding to a size of 64 kDa. (B) SEC-MALLS analysis of pA-VTX. The curves represent the RI elution profile of pA-VTX (blue) and BSA (black) overlaid with the scatter plot of the light-scattering estimated mass along the elution volume.

peptamer was conjugated to HRP using a 1:4 pA-VTX-to-HRP molar ratio (Supporting Information). The assay concentration of coating antibody and pA-VTX peroxidase were optimized by checkerboard titration, as described before,[9] and were used to develop the VTX-nanopeptamer ELISA for molinate. The dose–response curves had a typical sigmoid shape with signal saturation at a high concentration of analyte (Figure 4).

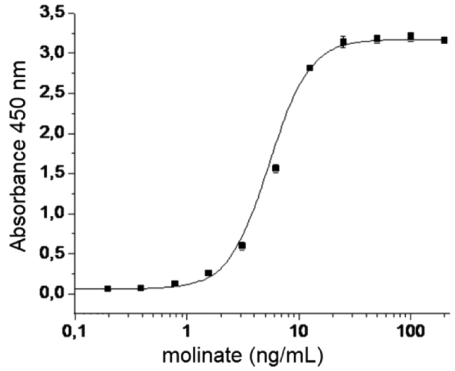

Figure 4. Noncompetitive ELISAs performed with the pA-VTX nanopeptamer. mAb14D7 (10 μg/mL) was used for coating, and pA-VTX (5 μg/mL) was added in the presence of increasing molinate concentrations. All measurements were performed in triplicate, and error bars represent the standard deviation.

However, as observed before with other PHAIA assays,[5,20] the slope was rather steep, limiting the dynamic range of the assay. This may be related to the multivalent nature of the interaction, which would rapidly increase as soon as the density of immunocomplexes on the solid phase increases along with the concentration of the analyte. The midpoint of the titration curve, corresponding to the concentration of analyte giving 50% of signal saturation (SC_{50}) was SC_{50} = 5.4 ± 0.3 ng/mL, and the limit of detection (LOD = analyte concentration giving a 10% increase over the zero signal) was 1.9 ng/mL for molinate.

These parameters were similar to those obtained with the phage-borne peptide, SC_{50} = 8.5 ± 0.2 ng/mL,[4] or with the streptavidin nanopeptamer prepared with commercial high-sensitivity streptavidin–HRP functionalized with the biotinylated synthetic peptide pA, SC_{50} = 8.3 ± 0.2 ng/mL, and LOD = 1.2 ng/mL.[9] This indicates that the spatial distribution of the peptides in the VTX nanopeptamer allows attainment of a similar avidity interaction with the immobilized IC than that achieved with the streptavidin or the phage display. Moreover, using the midpoint of the assay titration curve for comparison, the SC_{50} of the pA-VTX molinate assay was ~13-fold more sensitive than the IC_{50} (analyte concentration causing 50% inhibition) of the competitive ELISA set-up with the same antibody (IC50 69 ± 0.5 ng/mL).[17]

Transfer of Different Anti-IC Peptides from the Phage to the VTX-Nanopeptamers Does Not Affect Their Reactivity. To further test the versatility of VTX as a scaffold, we used the herbicide clomazone and its cognate antibody mAb 5.6 as an alternative model system. In a previous study,[16] we selected 18 phage clones against the clomazone/mAb 5.6 IC from a random 8-mer disulfide constrained library, which could be grouped into four peptide sequences (Table 1). Out of these sequences, the phage-borne peptide ICX11 produced the most sensitive PHAIA test. On the basis of the consensus sequence of those four peptides, we built a saturation mutagenesis library using the p8 V2 phagemid vector[21] to evolve peptides with higher affinity for the clomazone IC. The library (2×10^8 independent clones) had the generic sequence C*xxx*PN*x*E*x*C, where capital letters represent the invariant consensus residues

Table 1. Peptide Sequences Isolated from the Random and the Mutagenesis Libraries[a]

−C*xxxxxxxx*C− library			−C*xxx*PN*x*E*x*C− library	
clone	peptide	frequency	clone	peptide
ICX05	CISAPNMEAC	5	ICX12m	CPM**APNVEAC**
ICX09	CALAPNQEAC	4	ICX34m	CSF**APNVEAC**
ICX07	CTQFPNPEAC	9	ICX05m	CAT**APNVEAC**
ICX11	CLEAPNIEGC	2	ICX09m	CLE**APNVEAC**
			ICX31m	CAE**APNVEGC**
			ICX16m	CAL**APNVEAC**
			ICX03m	CLE**APNAEAC**
			ICX07m	CAQ**APNAEAC**
			ICX23m	CSW**APNAEAC**
			ICX20m	CTE**APNIEAC**
			ICX24m	CLF**APNIEAC**
			ICX30m	CPW**APNLEAC**
			ICX29m	CPA**APNLEAC**
			ICX18m	CTF**APNFEAC**

[a]Consensus residues of the panel of peptides isolated from the random library are shown in bold.

dx.doi.org/10.1021/ac500926f | Anal. Chem. 2014, 86, 5541–5546

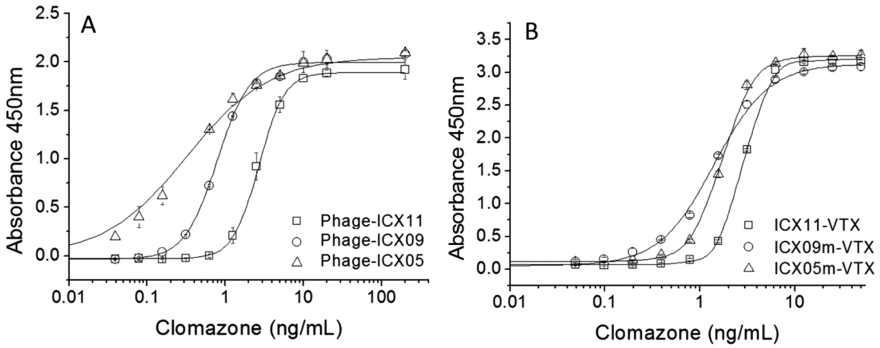

Figure 5. PHAIA and nanopeptamer assay for clomazone developed with the anti-immunocomplex peptides selected from the mutagenesis library. (A) Assay performed with the phage-borne peptides (PHAIA) or (B) with the peptide–VTX nanopeptamers conjugated to HRP. All measurements were performed in triplicate, and error bars represent the standard deviation.

and the "*x*" represents a fully randomized position. The selection of this library (Supporting Information) was performed against limiting amounts of the clomazone/mAb 5.6 IC, under stringent conditions (including a 5-day prolonged final washing step) to promote the isolation of a second generation of peptides with improved affinity for the IC, which could translate into better assay sensitivities. Fourteen clones were selected and are listed in Table 1.

A more complex consensus sequence emerged, with Ala in third and eighth positions, and a small hydrophobic residue (Val, Ala, Leu, Ile) in the sixth position. After a preliminary screening, two clones were selected that in the PHAIA format exhibited the highest SC_{50} differences (3–4-fold) with the phage-borne peptide ICX11 (Figure 5a, Table 2). Those two peptides, ICX05m and ICX09m, differed only in positions 1 and 2 and were used together with peptide ICX11 to compare changes in the assay performance when the peptides were moved from the phage to the VTX display. The assay performance of the VTX nanopeptamers built with these peptides is shown in Figure 5b and summarized in Table 2. There were no major differences between the PHAIA and the nanopeptamer assays, and despite the small drop in sensitivity in the case of ICX05m and ICX09m, it can be concluded that the VTX nanopeptamer–HRP conjugate can substitute for the phage particles, representing a convenient option for the development of noncompetitive assays for small molecules.

Table 2. Assay Parameters of the PHAIA and Nanopeptamer Formats

peptide ID	SC_{50} phage	SC_{50} nanopeptamer
ICX11	2.7 ± 0.1	2.9 ± 0.03
ICX09m	0.82 ± 0.01	1.4 ± 0.07
ICX05m	0.43 ± 0.2	1.7 ± 0.06

Good Recoveries Were Obtained When Different Water Samples Were Analyzed with the VTX Nanopeptamer Assay. Because of its sensitivity, the pICX09m-VTX HRP conjugate was used to assess the assay performance with real water samples spiked with clomazone. These samples comprised surface water samples collected from a region of Uruguay with no record of clomazone use, as well as mineral and tap water. The assay was performed with the addition of an "interference buffer" that contained a bulk protein (BSA), a chelating agent, and high salt concentration to avoid the matrix effect caused by humic acids and other interfering compounds in the samples. Under these conditions, undiluted samples could be directly analyzed with very good recoveries, even for the smallest concentrations tested, as is shown in Table 3.

The VTX Nanopeptamers Can Be Used to Set up Lateral-Flow Test with a Positive Readout. Lateral flow assays are a salient option as point of care tests because they are simple and fast and do not require specialized equipment. In addition, the formation of a colored test line over a white background is easily detected by the naked eye, making the test instrument-free. Unfortunately, competitive assays have to be developed into lateral-flow tests with a "negative" readout, in which the presence of the analyte causes an absence of signal, affecting its sensitivity and making its interpretation more difficult. We recently showed that nanopeptamers formed by the complex of avidin with biotinylated synthetic peptides could be used to develop a sensitive lateral-flow test with a positive readout.[9] This had not been possible with the use of phage-borne peptides, probably because of the filamentous structure of the M13 phage particles that may form aggregates upon labeling with carbon black, as has been reported when using colloidal gold.[22] To test whether the VTX scaffold could also allow the development of lateral flow tests, we labeled the pICX09m-VTX nanopeptamer with carbon black and evaluated the ability of the assay to detect low concentrations of the analyte. Figure 6 shows a typical result. The formation of a reaction line visible to the naked eye, as judged by four independent observers, was evident even for the lowest concentration assayed, 2.5 ng/mL. That was in agreement

Table 3. Recovery (%) from Spiked Samples Using the pICX09m-VTX Nanopeptamer Assay

clomazone (ng/mL)	Milli-Q water	tap water1	tap water 2	mineral water 1	mineral water 2	dam water 1	dam water 2	dam water 3	dam water 4
0.5	120 ± 10	85 ± 11	100 ± 5.0	130 ± 1.0	95 ± 10	129 ± 15	87 ± 13	110 ± 25	157 ± 5.0
1.0	112 ± 5.0	73 ± 9.3	128 ± 4.0	110 ± 10	103 ± 5.0	121 ± 5.0	91 ± 1.5	110 ± 10	119 ± 5.0
2.0	102 ± 5.0	87 ± 9.2	89 ± 10	110 ± 7.0	78 ± 5.0	83 ± 3.5	90 ± 18	102 ± 10	101 ± 10
2.5	93 ± 8.0	95 ± 2.9	100 ± 5.0	109 ± 4.0	78 ± 5.0	113 ± 5.0	115 ± 10	112 ± 10	94 ± 4.0
5.0	85 ± 3.0	93 ± 4.1	98 ± 20	124 ± 3.0	120 ± 20	114 ± 15	112 ± 6.0	96 ± 8.0	104 ± 5.0

dx.doi.org/10.1021/ac500926f | *Anal. Chem.* 2014, 86, 5541–5546

Densitometry analysis		
Clomazone (ng/mL)	Test line area	Control line area
0	119	4232
2.5	1905	4316
5.0	1272	4306
10	2995	4752
20	3898	4972
40	5479	4745

Figure 6. Noncompetitive nanopeptamer pICX09-VTX lateral-flow test for clomazone. The nitrocellulose strips were tested with buffer PBS containing various concentrations of clomazone (40, 20, 10, 5.0, 2.5, and 0 ng/mL) as denoted in the figure. The lower reaction line (test line) corresponds to the formation of the mAb5.6/clomazone/carbon-labeled pICX09-VTX trivalent complex, and the upper one (control line), to the interaction of the anti-HA antibody with carbon-labeled VHH-HA.

with the analysis by densitometry using the IMAGEJ software (NIH, USA).

CONCLUSIONS

The doughnut-like shape of the B1 subunit of the Shiga like toxin of *E. coli* offers a convenient option to multimerize binding domains with increased avidity. That was the case of the four anti-immunocomplex peptides used for noncompetitive detection of molinate and clomazone, in which it allowed the substitution of the phage particle ($900 \times 6-7$ nm, 1.6×10^7 Da) by oligomeric recombinant nanopeptamers of ~65 kDa, which constitute conventional and nonbiological immunoassay components. We recently showed that this was possible using biotinylated synthetic peptides and commercial avidins; however, the use of recombinant chimera that already includes the anti-immunocomplex peptide and self-assemble into a soluble multivalent complex of defined stoichiometry is a substantial step forward to make nanopeptamers simpler more affordable and easier to standardize. The fact that the VTX-nanopeptamers can be easily labeled with carbon black is also a major advantage because it allows the development of a lateral-flow test with a more intuitive positive readout, a feat that is not possible with the competitive format.

ASSOCIATED CONTENT

Supporting Information

Additional information as noted in the text. This material is available free of charge via the Internet at http://pubs.acs.org

AUTHOR INFORMATION

Corresponding Author

*Address: Av. A. Navarro 3051, piso 2, 11600 Montevideo, Uruguay. Phone: (598) 24874334. E-mail: ggonzal@fq.edu.uy.

Author Contributions

G.L. performed most of the experimental work. The manuscript was written through contributions of all authors. All authors have given approval to the final version of the manuscript.

Notes

The authors declare no competing financial interest.

ACKNOWLEDGMENTS

This work was supported with funds provided by Grants FMV 3138 ANII (Agencia Nacional de Investigación e Innovación, Uruguay) and TW05718 Fogarty Center NIH. G.L. is the recipient of an ANII scholarship.

REFERENCES

(1) Kobayashi, N.; Oyama, H. *Analyst* **2011**, *136*, 642−651.
(2) Lamminmaki, U.; Kankare, J. A. *J. Biol. Chem.* **2001**, *276*, 36687−36694.
(3) Monnet, C.; Bettsworth, F.; Stura, E. A.; Le Du, M. H.; Menez, R.; Derrien, L.; Zinn-Justin, S.; Gilquin, B.; Sibai, G.; Battail-Poirot, N.; Jolivet, M.; Menez, A.; Arnaud, M.; Ducancel, F.; Charbonnier, J. B. *J. Mol. Biol.* **2002**, *315*, 699−712.
(4) Gonzalez-Techera, A.; Vanrell, L.; Last, J. A.; Hammock, B. D.; Gonzalez-Sapienza, G. *Anal. Chem.* **2007**, *79*, 7799−7806.
(5) Gonzalez-Techera, A.; Kim, H. J.; Gee, S. J.; Last, J. A.; Hammock, B. D.; Gonzalez-Sapienza, G. *Anal. Chem.* **2007**, *79*, 9191−9196.
(6) Kim, H. J.; Rossotti, M. A.; Ahn, K. C.; Gonzalez-Sapienza, G. G.; Gee, S. J.; Musker, R.; Hammock, B. D. *Anal. Biochem.* **2010**, *401*, 38−46.
(7) Carlomagno, M.; Mathó, C.; Cantou, G.; Sanborn, J.; Last, J.; Hammock, B.; Roel, A.; González, D.; González-Sapienza, G. . *J. Agric. Food Chem.* **2010**, *58*, 4367−4371.
(8) Kim, H. J.; McCoy, M.; Gee, S. J.; Gonzalez-Sapienza, G. G.; Hammock, B. D. *Anal. Chem.* **2011**, *83*, 246−253.
(9) Vanrell, L.; Gonzalez-Techera, A.; Hammock, B. D.; Gonzalez-Sapienza, G. *Anal. Chem.* **2013**, *85*, 1177−1182.
(10) Falnes, P. O.; Sandvig, K. *Curr. Opin. Cell Biol.* **2000**, *12*, 407−413.
(11) Stein, P. E.; Boodhoo, A.; Armstrong, G. D.; Cockle, S. A.; Klein, M. H.; Read, R. J. *Structure* **1994**, *2*, 45−57.
(12) Lingwood, C. A.; Law, H.; Richardson, S.; Petric, M.; Brunton, J. L.; De Grandis, S.; Karmali, M. *J. Biol. Chem.* **1987**, *262*, 8834−8839.
(13) Conrady, D. G.; Flagler, M. J.; Friedmann, D. R.; Vander Wielen, B. D.; Kovall, R. A.; Weiss, A. A.; Herr, A. B. *PloS One* **2010**, *5*, e15153.
(14) Stone, E.; Hirama, T.; Tanha, J.; Tong-Sevinc, H.; Li, S.; MacKenzie, C. R.; Zhang, J. *J. Immunol. Methods* **2007**, *318*, 88−94.
(15) Zhang, J.; Tanha, J.; Hirama, T.; Khieu, N. H.; To, R.; Tong-Sevinc, H.; Stone, E.; Brisson, J. R.; MacKenzie, C. R. *J. Mol. Biol.* **2004**, *335*, 49−56.
(16) Rossotti, M. A.; Carlomagno, M.; González-Techera, A.; Hammock, B. D.; Last, J.; González-Sapienza, G. *Anal. Chem.* **2010**, *82*, 8838−8843.
(17) Rufo, C.; Hammock, B. D.; Gee, S. J.; Last, J. A.; Gonzalez-Sapienza, G. *J. Agric. Food Chem.* **2004**, *52*, 182−187.
(18) Olichon, A.; Schweizer, D.; Muyldermans, S.; de Marco, A. *BMC Biotechnol* **2007**, *7*, 7.
(19) Wen, J.; Arakawa, T.; Philo, J. S. *Anal. Biochem.* **1996**, *240*, 155−166.
(20) Rossotti, M. A.; Carlomagno, M.; Gonzalez-Techera, A.; Hammock, B. D.; Last, J.; Gonzalez-Sapienza, G. *Anal. Chem.* **2010**, *82*, 8838−8843.
(21) Cwirla, S. E.; Dower, W. J.; Li, M. *Methods Mol. Biol.* **1999**, *128*, 131−141.
(22) Souza, G. R.; Christianson, D. R.; Staquicini, F. I.; Ozawa, M. G.; Snyder, E. Y.; Sidman, R. L.; Miller, J. H.; Arap, W.; Pasqualini, R. *Proc. Natl. Acad. Sci. U.S.A.* **2006**, *103*, 1215−1220.